A Chebyshev method for a free boundary problem modeling tumor growth

Wenrui Hao[*] Oliver Kernell[†] Andrew Sommese[‡]

May 23, 2013

1 Mathematical model

Mathematical models of tumor growth, which consider the tumor tissue as a density of proliferating cells, have been developed and studied in many papers; see [1, 2, 4, 5, 6, 7, 8, 9, 16, 17] and the references given there. Most of the models discuss the case of radially symmetric tumors. Since tumors grown in vitro have a nearly spherical shape, it is important to determine whether these radially symmetric tumors are asymptotically stable.

While tumors grown in vitro have a nearly spherical shape, tumors grown in vivo are usually not. It is therefore also very interesting to study what will happen for the non-radially symmetric tumors.

Let $\Omega(t)$ denote the tumor region, σ denote the concentration of nutrients, p denote the pressure, $\widetilde{\sigma}$ denote the concentration of nutrients needed for sustainability, and μ denote the aggressiveness of the tumor. Let κ denote the mean curvature, n denote the outward normal direction, and V_n denote the velocity of $\partial\Omega(t)$ in the outward normal direction n. A normalized model of a free boundary problem for a system of PDEs modeling tumor growth is

[*]Department of Applied and Computational Mathematics and Statistics, University of Notre Dame, Notre Dame, IN 46556 (whao@nd.edu, www.nd.edu/∼whao).

[†]Department of Applied and Computational Mathematics and Statistics, University of Notre Dame, Notre Dame, IN 46556 (okernell@nd.edu).

[‡]Department of Applied and Computational Mathematics and Statistics, University of Notre Dame, Notre Dame, IN 46556 (sommese@nd.edu, www.nd.edu/∼sommese).

given by

$$\begin{cases} \sigma_t - \Delta\sigma &= -\sigma & \text{in } \Omega(t) \\ -\Delta p &= \mu(\sigma - \widetilde{\sigma}) & \text{in } \Omega(t) \\ \\ \sigma &= 1 & \text{on } \partial\Omega(t) \\ p &= \kappa & \text{on } \partial\Omega(t) \\ \frac{\partial p}{\partial n} &= -V_n & \text{on } \partial\Omega(t). \end{cases}$$

The above model of tumor growth assumes that the tumor region $\Omega(t)$ contains just one type of cells with density c which is proportional to the nutrient concentration σ. Here p is the pressure which results from cell proliferation. It is also assumed in this model that the cell density grows according to the proliferation rate $\mu(\sigma - \widetilde{\sigma})$ where $\widetilde{\sigma}$ is a constant smaller than the concentration of nutrients on the boundary, that is, $\widetilde{\sigma} < 1$. This linear approximation is the result of first order Taylor expansion for the fully nonlinear model. In deriving this system, the tumor region is assumed to be a porous medium like material, so that Darcy's law $\vec{V} = -\nabla p$ holds. Together with the law of conservation of mass $\mathrm{div}\vec{V} = \mu(\sigma - \widetilde{\sigma})$ yields the equations in the model.

Radially symmetric solutions are known to exist for both the 2-dimensional and 3-dimensional steady-state system. It is known that there exists values of μ, denoted μ_ℓ for $\ell \geq 2$, where branches of nonradially symmetric solutions intersect the set of radially symmetric solutions. It is shown that the nonradially symmetric solutions exist along a branch at μ_ℓ.

Note that these results are valid only in a small neighborhood of the bifurcation branching point. A very challenging question is to find out what happens if the parameters *go beyond this small neighborhood.* It is clear that numerical computation is needed to answer these questions. In particular, it is very interesting to find out whether it is possible for the tumor to grow into other shapes such as dumb-bell shape, indicating the spreading of the cancer.

To demonstrate the ability of numerical computational methods applied to free boundary problems, we setup a polynomial system to compute μ_ℓ and track along the solution branch of nonradially symmetric solutions in the 2-dimensional steady-state system. Due to the free boundary, we developed a chebyshev's method, which is based on polar coordinates and allows the length of the radii in each direction to change independently. This new method shows efficiency than existing numerical methods [10, 11, 12, 13, 14, 15].

2 Radially symmetric stationary solutions

In this paper, we will only consider the two space dimensional case. The three dimensional case can be considered in a similar way. Solving

$$\sigma_{rr} + \frac{1}{r}\sigma_r = \sigma, \sigma(R) = 1,$$

we obtain

$$\sigma_s(r) = \frac{I_0(r)}{I_0(R)}, \tag{2.1}$$

where $I_n(r)$ is the modified bessel function. Solving

$$-\Delta(p + \mu\sigma) = -\mu\widetilde{\sigma}, (p + \mu\sigma)(R) = \frac{1}{R} + \mu,$$

we obtain

$$p_s(r) = -\mu\sigma_s(r) + \frac{\mu\widetilde{\sigma}}{4}(r^2 - R^2) + \frac{1}{R} + \mu. \tag{2.2}$$

The boundary condition

$$\frac{\partial p_s}{\partial r}(R) = 0$$

yields the formula of $\widetilde{\sigma}$, i.e.,

$$\widetilde{\sigma} = \frac{2I_1(R)}{RI_0(R)}. \tag{2.3}$$

Lemma 2.1. *For any given $\mu > 0$ and $0 < \widetilde{\sigma} < 1$, there exists a unique stationary solution $(\sigma_s(r), p_s(r), R)$ is given by (2.1) and (2.2) where R is uniquely determined by (2.3).*

Proof. We denote $f(R) = \frac{2I_1(R)}{RI_0(R)}$, which satisfies

$$\lim_{R\to 0} f(R) = 1, \lim_{R\to\infty} f(R) = 0,$$

and $f'(R) < 0 \forall R$. Then $f(R)$ has a unique solution for each $\widetilde{\sigma} \in (0, 1)$. □

3 Bifurcation from radially symmetric stationary solution

We now turn our attention to computing nonradially symmetric stationary solutions of the form

$$
\begin{aligned}
&& \sigma &= \sigma_s + \epsilon\sigma_1 + O(\epsilon^2),\\
&& p &= p_s + \epsilon p_1 + O(\epsilon^2),\\
\partial\Omega_\epsilon : && r &= R + \epsilon S(\theta) + O(\epsilon^2),
\end{aligned}
$$

In order to compute the Frechét derivative in the direction $S(\theta)$, we first formally compute σ_1 and p_1.

Computation of σ_1: Clearly,

$$
\epsilon\sigma_1|_{\partial B_R} \quad = \quad \epsilon\sigma_1|_{\partial\Omega_\epsilon} + O(\epsilon^2) = 1 - \sigma_s(R+\epsilon S) + O(\epsilon^2) = -\epsilon\sigma_s'(R)S(\theta) + O(\epsilon^2).
$$

Thus, after dropping higher terms,

$$
\begin{cases}
-\Delta\sigma_1 + \sigma_1 = 0 & \text{in } B_R,\\
\sigma_1 = -\sigma_s'(R)S & \text{on } \partial B_R,
\end{cases}
$$

It follows that, for $S(\theta) = \cos(l\theta), l = 2, 3, 4, 5, \cdots$, by separation of variables

$$
\sigma_1(r) = -\sigma_s'(R)\cos(l\theta)\frac{I_l(r)}{I_l(R)}. \tag{3.4}
$$

Computation of p_1: By linearizing the mean curvature κ, we have

$$
\kappa = \frac{1}{R} - \frac{\epsilon}{R^2}(S + S'') + O(\epsilon^2). \tag{3.5}
$$

After dropping higher terms, we have, in each of the respective (tumor region, necrotic region) region,

$$
\begin{cases}
-\Delta p_1 = \mu\sigma_1 & \text{in } B_R,\\
p_1 = -p_s'(R)S - \frac{1}{R^2}(S + S'') & \text{on } \partial B_R.
\end{cases}
$$

Since $p_s'(R) = 0$, and in the case $S = \cos(l\theta)$, we obtain

$$
\begin{cases}
-\Delta(p_1 + \mu\sigma_1) = 0 & \text{in } B_R,\\
p_1 + \mu\sigma_1 = (-\frac{1}{R^2} - \mu\sigma_s'(R) + \frac{l^2}{R^2})\cos(l\theta) & \text{on } \partial B_R.
\end{cases}
$$

Thus,

$$p_1 + \mu\sigma_1 = (-\frac{1}{R^2} - \mu\sigma_s'(R) + \frac{l^2}{R^2})\frac{r^l}{R^l}\cos(l\theta). \tag{3.6}$$

For each $S(\theta)$ and μ, define

$$F(S,\mu) = \frac{\partial p}{\partial n}\Big|_{\partial\Omega_\epsilon}. \tag{3.7}$$

Then S induces an stationary solution if and only if $F(S,\mu) = 0$. Clearly

$$\frac{\partial p}{\partial n}\Big|_{r=R+\epsilon S} = \epsilon\left(\frac{\partial^2 p_s(R)}{\partial r^2}S + \frac{\partial p_1}{\partial r}\right) + O(\epsilon^2). \tag{3.8}$$

Thus, formally, the Frechét derivative in the direction $\cos(l\theta)$ is given by

$$\left[\frac{\partial F}{\partial S}(0,\mu)\right]\cos(l\theta) = \frac{\partial^2 p_s(R)}{\partial r^2}\cos(l\theta) + \frac{\partial p_1}{\partial r}. \tag{3.9}$$

We claim that the condition for bifurcation is

$$\left[\frac{\partial F}{\partial S}(0,\mu)\right]\cos(l\theta) \equiv 0, \tag{3.10}$$

and this will determine $\mu = \mu_l$. We now proceed to rigorously derive this. From (2.2), we have

$$\frac{\partial^2 p_s(R)}{\partial r^2} = \mu\Big(-\frac{\partial^2\sigma_s(R)}{\partial r^2} + \frac{I_1(R)}{RI_0(R)}\Big). \tag{3.11}$$

Using the formula for p_1

$$\frac{\partial p_1}{\partial r}(R) + \mu\frac{\partial\sigma_1}{\partial r}(R) = (-\frac{1}{R^2} - \mu\sigma_s'(R) + \frac{l^2}{R^2})\frac{l}{R}\cos(l\theta). \tag{3.12}$$

Substituting $\frac{\partial\sigma_1}{\partial r}(R)$ into (3.12) and using (3.9) and (3.10), we find

$$\mu\Big(-\frac{\partial^2\sigma_s(R)}{\partial r^2} + \frac{I_1(R)}{RI_0(R)} + \frac{\sigma_s'(R)}{I_l(R)}I_l'(R) - \frac{l}{R}\sigma_s'(R)\Big) - \frac{l}{R^3} + \frac{l^3}{R^3} = 0.$$

Thus $A_l \cdot \mu_l - B_l = 0$ if $A_l \neq 0$, then $\mu_l = \dfrac{B_l}{A_l}$, where

$$A_l = 1 - \frac{2I_1(R)}{RI_0(R)} - \frac{I_1(R)}{I_0(R)}\left(\frac{I_l'(R)}{I_l(R)} - \frac{l}{R}\right) \doteq \alpha + \beta_l \tag{3.13}$$

$$B_l = \frac{l^3 - l}{R^3}. \tag{3.14}$$

From [10], we apply the Crandall-Rabinowitz theorem and get the following lemma.

Lemma 3.1. $\mu_2 < \mu_3 < \mu_4 < \cdots$.

4 Numerical methods

We begin creating the numerical method by first establishing a circular grid by which we can compute the points within the boundary and model the shape of the tumor. With previous methods, points were evenly spaced apart along the radii, and the radii were spaced evenly through a theta angle. This method wastes valuable computation time on the interior of the tumor which is of little concern to the solution. The new method utilizes Chebyshev Polynomials to determine spacing. This groups more points closer to the boundary where the majority of the computation is needed. The equation governing this spacing is

$$R\cos(i * \pi/N_r), \tag{4.15}$$

where R equals the size of the radius, i is the step, and N_r is the number of gridpoints.

Then a stencil is fitted to the grid to compute the interior values of the tumor model. We utilized a 3rd order finite difference scheme for the interior and boundary points. This scheme has points placed along the r-axis and theta-axis as shown below.

As the scheme is tracked to the last two boundary points, on each radius, the right most points are shifted to the opposite side, as indicated in the figure.

A primary tool used in the tracking of μ is the software Bertini. Bertini utilizes homotopy method as a way to track points from an equation where known solutions exits to an equation that is similar but the solutions are

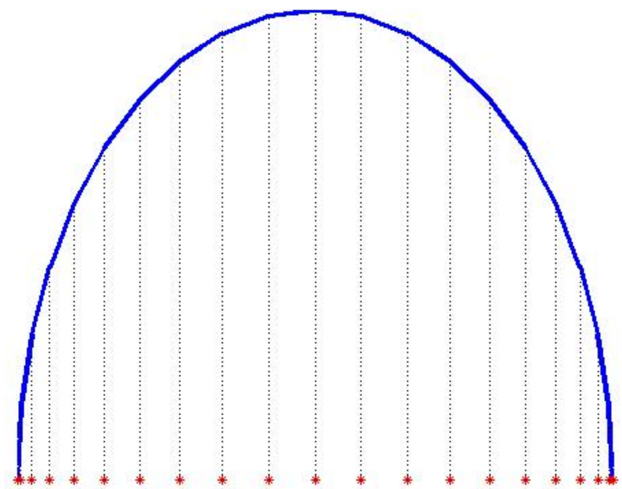

Figure 1: Chebyshev mapping to generate gridpoints in R direction from the unit circle.

unknown. This is expressed in the equation $H(x,t) = f(x) * t + g(x) * (1-t)$ where $f(x)$ is the know function and $g(x)$ is the unknown function. The variable t is then tracked from 0 to 1.

Often times regions of the homotopy function $H(x,t)$ becomes unstable. In this case, higher precision is required. Fortunately, Bertini features multi-precision tracking which increases the number of digits when higher precision is required. This allows for faster tracking in stable regions with less digits and high precision tracking in unstable regions. Multi-precision is also used near singularities in the homotopy function. plot a figure **??**

As Bertini tracks μ along its radially symmetric path, its values are plotted. In order to find where μ bifurcates, the condition number of the jacobian is computed and graphed. Bifurcations occur near where the condition number is at its maximum values.

At this bifurcation, we want to find the nonradial solution path. In order to do this, the tangent cone was computed to approximate the numerical value for a point on the nonradial path. **explain how to compute the tangent cone** Once an approximate solution was produced, Bertini was used to begin tracking to find the nonradial path. The upper and lower

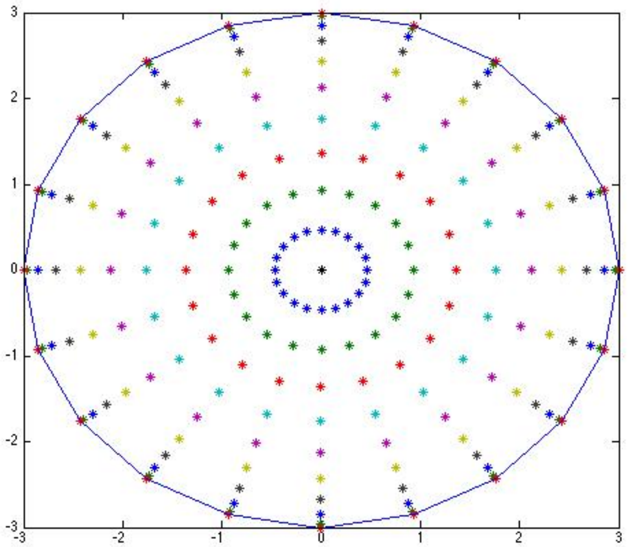

Figure 2: Entire grid using Chebyshev's Method.

branches shown in figure **??** were not discovered by previous methods.

You can write an algorithm to show the procedure of the computing. Please use algorithm2e to write it. http://mirror.hmc.edu/ctan/macros/latex/

5 Numerical results

Table 1: Timing Results: Paths tracked from $\mu = 1.7$ to $\mu = 1.9$

	Number of points	Chebyshev Method	Previous method
Top Path	n	3918.389206s	5
Top Path	2n	74210.596403s	5
Bottom Path	n	3882.229745s	5

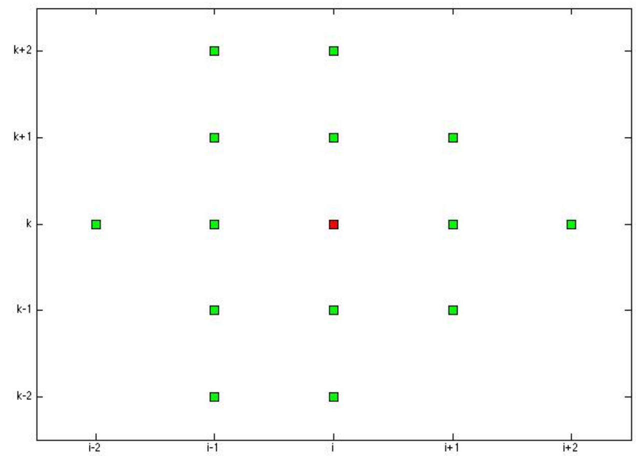

Figure 3: Scheme with the red point as the center point (i,k).

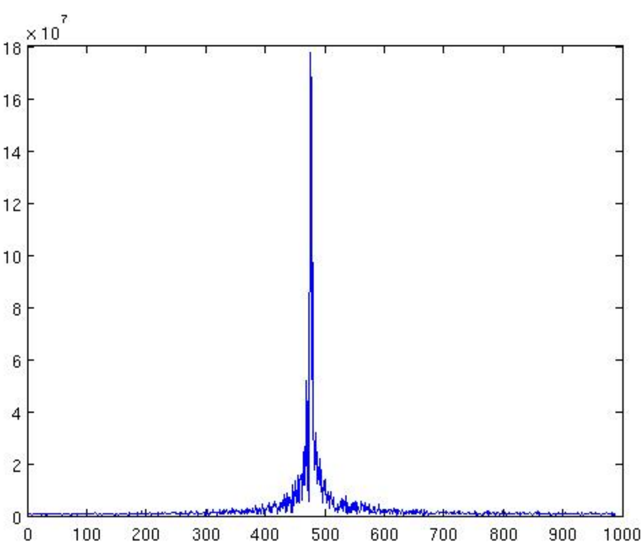

Figure 4: Condition Number.

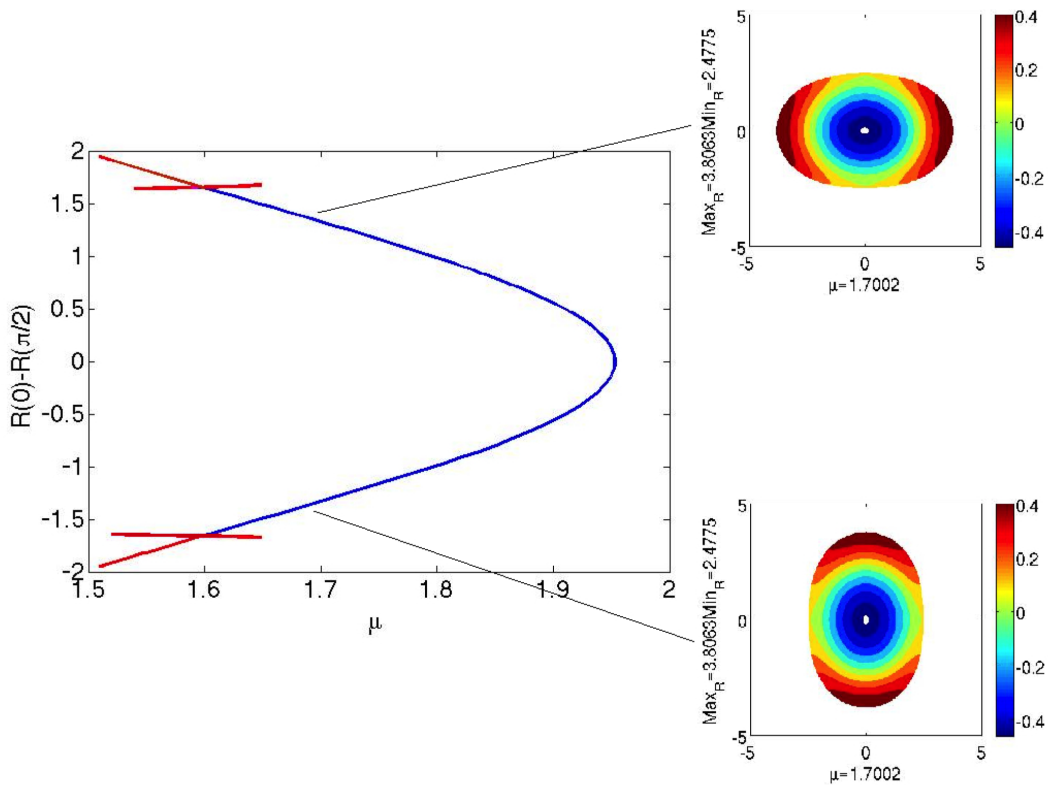

Figure 5: Solution behavior with blue lines indicating paths previously discovered and red lines indicating newly discovered paths.

References

[1] J.A. Adam, General aspect of modeling tumor growth and immune response, A Survey of Models for Tumor-Immune System Dynamics (J.A.Adam and N. Bellomo, eds.) Birkhäuser, Boston, 14-87, (1996).

[2] J.A. Adam and S.A. Maggelakis, Diffusion regulated growth characteristics of a spherical prevascular carcinoma, *Bull. Math. Biol.*, Vol 52, 549-582, (1990).

[3] D.J. Bates, J.D. Hauenstein, A.J. Sommese, and C.W. Wampler, Bertini: Software for numerical algebraic geometry. Available at www.nd.edu/∼sommese/bertini.

Table 2: μ Comparison

Theoretical Value	Chebyshev Method	Previous method
1.9533	1.9520	5

[4] B. Bazally and A. Friedman, A free boundary problem for elliptic-parabolic system: Application to a model of tumor growth, *Comm. Partial Diff. Eq.*, Vol 28, 517-560, (2003).

[5] N. Britton and M.A.J. Chaplain, A qualitative analysis of some models of tissue growth, *Math. Biosci.*, Vol 113, 77-89, (1993).

[6] H.M. Byrne, The importance of intercellular adhesion in the development of carcinomas, *IMA J. Math. Appl. Med. Biol.*, Vol 14, 305-323, (1997).

[7] H.M. Byrne and M.A.J. Chaplain, Growth of nonnecrotic tumors in the presence and absence of inhibitors, *Math. Biosci.*, Vol 135, 187-216, (1996).

[8] A. Friedman and B. Hu, Bifurcation from stability to instability for a free boundary problem arising in a tumor model *Arch. Rat. Mech. Anal.*, Vol. 180, No. 2, (2006).

[9] A. Friedman and B. Hu, Stability and instability of Liapunov-Schmidt and Hopf bifurcation for a free boundary problem arising in a tumor model. *Trans. Amer. Math. Soc.*, Vol 360, 5291–5342, (2008).

[10] W. Hao, J.D. Hauenstein, B. Hu, Y. Liu, A.J. Sommese, and Y.-T. Zhang, Bifurcation of steady-state solutions for a tumor model with a necrotic core, *Nonlinear Analysis Series B: Real World Applications*, Vol. 13, 694–709, (2012).

[11] W. Hao, J.D. Hauenstein, B. Hu, Y. Liu, A.J. Sommese, and Y.-T. Zhang, Continuation along bifurcation branches for a tumor model with a necrotic core, *Journal of Scientific Computing*, Vol. 53, 395–413, (2012).

[12] W. Hao, J.D. Hauenstein, B. Hu, and A.J. Sommese, A three-dimensional steady-state tumor system, *Applied Mathematics and Computation*, Vol. 218, 2661–2669, (2011).

[13] W. Hao, J.D. Hauenstein, B. Hu, and A.J. Sommese, A domain decomposition algorithm for computing multiple steady states of differential equations, *submitted: available at www.nd.edu/∼whao/publication.html*.

[14] W. Hao, J.D. Hauenstein, B. Hu, T. McCoy and A.J. Sommese, Computing steady-state solutions for a free boundary problem modeling tumor growth by Stokes equation, *Journal of Computational and Applied Mathematics*, Vol. 237, 326–334, (2013).

[15] W. Hao, B. Hu and A. J. Sommese, Cell cycle control and bifurcation for a free boundary problem modeling tissue growth, *submitted*.

[16] S.A. Maggelakis and J.A. Adam, Mathematical model for prevasculat growth of a spherical carcinoma, *Math. Comp. Modeling*, Vol 13, 23-38, (1990).

[17] D.L.S. McEwain and L.E. Morris, Apoptosis as a volume loss mechanism in mathematical models of solid tumor growth, *Math. Biosci.*, Vol 39, 147-157, (1978).